

Adsorption of AR114 onto humic acid-modified Fe₃O₄ nanoparticles

DOI: 10.35530/IT.074.06.20233

GÜL KAYKIOĞLU
DERMAN VATANSEVER BAYRAMOL

AYLIN YILDIZ

ABSTRACT – REZUMAT

Adsorption of AR114 onto humic acid-modified Fe₃O₄ nanoparticles

In this study, Fe₃O₄ and humic acid-modified Fe₃O₄ (Fe₃O₄@HA) magnetic nanoparticles were synthesized and used for the removal of Acid Red 114 (AR114) dyestuff from aqueous. The batch adsorption method was used for the experiments. The magnetic nanoparticles, synthesised by an inexpensive and environmentally friendly precipitation process, were characterised by FTIR, SEM-EDX, BET surface area, and XRD analyses. The optimum pH values determined for Fe₃O₄ and Fe₃O₄@HA were the original pH (6.4) and 4, respectively. The equilibrium state was reached after 60 minutes for both adsorbents. The values for Fe₃O₄ and Fe₃O₄@HA were determined as 3.4 mg/g and 3.1 mg/g, respectively, when 10 mg/l initial dyestuff concentration and 2 g adsorbent were used. The results obtained in the adsorption experiments performed for both adsorbents were compatible with the Freundlich isotherm and pseudo-second-order kinetic model. Fe₃O₄ was found to be more efficient than Fe₃O₄@HA in terms of reuse and Fe₃O₄ can be used 5 times without any significant loss of adsorption capacity. The results showed that Fe₃O₄ and Fe₃O₄@HA can be environmentally friendly alternative adsorbents for the removal of hazardous azo dyestuffs from water, and have regeneration possibilities.

Keywords: Acid Red 114, adsorption, colour removal, Fe₃O₄, humic acid, magnetic nanoparticle

Adsorbția AR114 pe nanoparticule de Fe₃O₄ modificate cu acid humic

În acest studiu, Fe₃O₄ și nanoparticulele magnetice Fe₃O₄ modificate cu acid humic (Fe₃O₄@HA) au fost sintetizate și utilizate pentru îndepărtarea colorantului Acid Red 114 (AR114) din soluție apoasă. Pentru experimente a fost utilizată metoda de adsorbție în loturi. Nanoparticulele magnetice, sintetizate printr-un proces de precipitare ieftin și prietenos cu mediul, au fost caracterizate prin analize FTIR, SEM-EDX, suprafață BET și XRD. Valorile optime ale pH-ului determinate pentru Fe₃O₄ și Fe₃O₄@HA au fost pH-ul inițial (6,4) și, respectiv, 4. Starea de echilibru a fost atinsă după 60 de minute pentru ambii adsorbânți. Valorile q_e pentru Fe₃O₄ și Fe₃O₄@HA au fost determinate la 3,4 mg/g și, respectiv, 3,1 mg/g, atunci când a fost utilizată o concentrație inițială de colorant de 10 mg/l și 2 g adsorbant. Rezultatele obținute în experimentele de adsorbție efectuate pentru ambii adsorbânți au fost compatibile cu izoterma Freundlich și modelul cinetic de pseudo-ordin doi. Fe₃O₄ s-a dovedit a fi mai eficient decât Fe₃O₄@HA în ceea ce privește reutilizarea, iar Fe₃O₄ poate fi utilizat de 5 ori fără nicio pierdere semnificativă a capacității de adsorbție. Rezultatele au arătat că Fe₃O₄ și Fe₃O₄@HA pot fi adsorbânți alternativi ecologici pentru îndepărtarea coloranților azoici periculoși din apă și au posibilități de regenerare.

Cuvinte-cheie: Acid Red 114, adsorbție, îndepărtare a culorii, Fe₃O₄, acid humic, nanoparticule magnetice

INTRODUCTION

Colour prevents light permeability in receiving environments, negatively affects photosynthetic activity, and can cause toxicity in aquatic organisms [1]. Today, methods such as physicochemical processes, membrane systems, and advanced oxidation processes are applied to remove the colour from wastewater [2], while one of the most effective ones is adsorption. In adsorption applications, it is important that the adsorbent used is low-cost, can be easily removed from the water environment, is suitable for reuse, and can be regenerated.

Magnetic nanoparticles are one of the most important adsorbents developed in recent years. Some of their

advantages are having large surface areas, high magnetic properties, high removal efficiencies, and easy and fast separation of adsorbent from solution (via magnetic field). In addition, adsorbed pollutants can be separated from magnetic nanoparticles and the adsorbent can be reused [3]. In recent years, iron-based nanoparticles have been widely used in environmental applications. Pan et al. [4] demonstrated the effectiveness of organic acid coatings on the Fe₃O₄ surface in preventing nanoparticles from aggregating in solution and metal adsorption. In various studies, Fe₃O₄ has been used by modifying it with organic substances such as chitosan, humic acid and alginate for the removal of pollutants [5, 6].

Rashid et al. [7] stated that the coating of natural organic materials on the magnetic nanoparticle surface can show lower toxic effects and more environmentally friendly properties. Such thin coatings can prevent aggregation and autoxidation that can be encountered with the use of magnetic nanoparticles alone. In addition, when magnetic nanoparticles are coated with natural organic matter, the potential in adsorption capacity and the selectivity of the nanoparticle increase. Humic acid (HA) is a natural organic macromolecule that is abundant in the world. The high reaction activity of HA is a result of its unique amorphous structure. This is due to the presence of large polycyclic aromatic hydrocarbons and many carboxyls, ether and amino groups in its skeleton [6]. These substances in their structure can show complex properties with types of metal oxides [7]. However, separating HA from the aquatic environment is difficult. For this reason, adsorption with a combination of HA and iron oxide is a promising approach, and the magnetic separation method can be used to separate adsorbents from the water environment. HA is stable at low pH (pH<3) but dissolves at pH>3. This limits the pH range of adsorption. Fe₃O₄@HA is formed by a bond formed between the Fe ions of Fe₃O₄ and the carboxylate groups of HA [8]. By modifying Fe₃O₄ with HA, adsorption can be applied in a wider pH range. As a result of the HA coating on Fe₃O₄, a reduction in the particle size of the adsorbent is expected [8, 9].

In recent years, there have been adsorption studies on the removal of various pollutants using Fe₃O₄@HA in various studies [6–8, 10–12].

One of the studies in which the adsorbent obtained by coating Fe₃O₄ with humic acid was used for colour removal and it was used for the adsorption of methylene blue (MB) from aqueous solutions. They determined that humic acid-coated Fe₃O₄ performed higher MB adsorption than Fe₃O₄ alone. It was determined that the adsorption was compatible with the pseudo-second-order kinetic model, the adsorption isotherm was compatible with the Langmuir model, and the maximum adsorbance amount was 0.291 mmol/g [6]. Rashid et al. synthesized humic acid-coated magnetic nanoparticles and used them for phosphate removal in aqueous media. The optimum pH of 6.6 and maximum adsorption capacity were determined as 28.9 mg/g. Adsorption behaviours were found to be compatible with Freundlich isotherm, Adsorption kinetics were compatible with the pseudo-second-order model [7]. Koesnapardi et al. evaluated phenol adsorption with HA-coated Fe₃O₄ coated with HA at different rates in their study. The optimum pH 5.0 for phenol adsorption is consistent with the pseudo-second-order kinetic model, the adsorption isotherm is compatible with the Langmuir model, and the maximum adsorbance amount is 0.45 mol/g was determined [8]. Peng et al. synthesized Fe₃O₄/HA nanoparticles and used them for Rhodamine B dye removal from aqueous solutions. Rhodamine B adsorption takes less than 15 minutes

to reach equilibrium. It is compatible with the Langmuir adsorption model and its q_{max} is 161.8 mg/g. The optimum pH was determined as (2.53) [12]. However, as a result of the literature search, no study was found on the removal of AR114 from aqueous solutions. In this study, Fe₃O₄ and humic acid-modified Fe₃O₄ (Fe₃O₄@HA) magnetic nanoparticles were synthesized and used for the removal of Acid Red 114 (AR114) dyestuff from aqueous.

MATERIAL AND METHOD

Preparation of Fe₃O₄ and Fe₃O₄@HA

FeCl₃·2H₂O and FeCl₂·4H₂O (2/1 mol) were dissolved in 50 mL of distilled water. During the preparation of Fe₃O₄@HA, 0.2 g of HA was also added. The solution was stirred rapidly (40°C) for 15 minutes. Then, by slowly adding NH₃, the pH was increased above 11 and ferritin was precipitated. In the next step, it was treated with argon gas, and reflux was made at 80°C with continuous stirring for 2 hours. Finally, the separation of Fe₃O₄ or Fe₃O₄@HA from the aqueous solution was accomplished with a strong magnet. The magnetic nanoparticles obtained were washed with distilled water several times and dried at 80°C for 4 hours in an oven [13].

Adsorbate and adsorption experiments

C.I. Acid Red 114 (AR 114), used as the adsorbate, was obtained from Sigma-Aldrich. AR114 is mainly used for dyeing textiles such as wool, silk, jute and leather [14, 15]. The molecular formula is C₃₇H₂₈N₄O₁₀S₃₂Na, and it is a dark red powder dye in the diazo chromophore group. Batch adsorption experiments were carried out in an orbital shaker and at constant agitating speed (200 rpm) at room temperature (25°C). In the adsorption studies, firstly, the effect of different pH values (4, 7, 9 and original pH (6.4)) was evaluated. Subsequent adsorption experiments were carried out at optimum pH. The effect of contact time (with samples taken after 0, 1, 5, 15, 30, 60, 90, 120 and 150 minutes) and the effect of initial dyestuff concentration (with 4, 6, 10 and 15 mg/l initial dyestuff concentration) were determined for both adsorbents. pH adjustment in the dyestuff solution was made with 0.1 N NaOH and 0.1 N HCl. The adsorbent was separated by a strong magnet, then colour measurement was performed in a spectrophotometer. While working at natural pH (original pH), no pH correction was made in the sample. The adsorption capacity (q_t , mg/g) in the adsorption experiments was determined by the following equations (equation 1). Where, C_0 (mg/l) is the initial AR114² concentration, C_e (mg/l) is the AR114 concentration in solution at equilibrium, m (g) is the adsorbent mass, and V (l) is the solution volume.

$$q_t = \frac{(C_0 - C_e) \cdot V}{m} \quad (1)$$

Damasceno et al. studied previously the dye adsorption of Fe₃O₄ and the interaction between the dye

molecules and Fe_3O_4 [16]. The interaction between the dyestuff and $\text{Fe}_3\text{O}_4@HA$ can be explained as dye molecules are trapped between the OH groups of HA in the structure of $\text{Fe}_3\text{O}_4@HA$ nanoparticles as shown in figure 1.

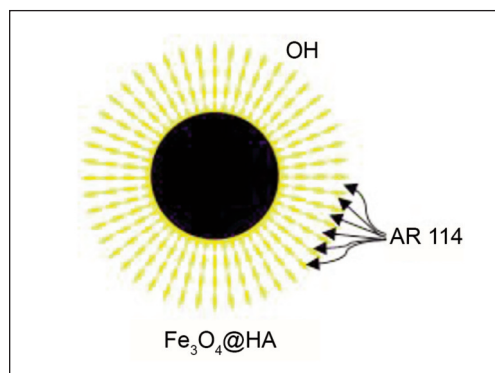


Fig. 1. Interaction between AR 114 dye molecules and $\text{Fe}_3\text{O}_4@HA$ nanoparticles

Desorption and reuse experiments

After the adsorption experiments, the desorption process was applied to the contaminated adsorbents. In the desorption application, 0.1 g of contaminated adsorbent was added to 50 ml of 9/1 (v/v) methanol/ acetic acid solution and shaken. Then the adsorbent is magnetically separated from the solution. The process was repeated until the amount of dyestuff in the solution was less than 0.002 mmol/L. Finally, the adsorbent was washed with distilled water and dried in an oven [17]. Reuse studies were carried out for Fe_3O_4 and $\text{Fe}_3\text{O}_4@HA$ at optimum pH conditions and within 60 minutes of contact time. Reuse studies were investigated with 7 repetitions.

Analysis

BET surface area was determined with the Quantachrome Quadrasorb SI instrument based on the nitrogen (N_2) gas adsorption technique. SEM-EDX examination was performed with the FEI Quanta FEG 250 model device. In the Bruker Vertex 70 FTIR ATR brand device, descriptive information about the bonds in the structures of the adsorbents was obtained with the ATR technique. XRD analyses were performed on the Panalytical Empyrean instrument. Colour parameter analyses were performed according to the maximum absorbance method by the Thermospectronic Aquamate Spectrometer. Accordingly, scans were made in the spectrometer at wavelengths between 400 nm and 700 nm and the wavelength with the highest absorbance was determined. Colour analyses were performed at 522 nm for AR114.

The pH_{pzc} was determined by adjusting the 0.01 mol/l NaCl solution to different pH values (with 0.1 N NaOH and 0.1 N HCl). It was shaken at room temperature for two days with the lid closed after 0.01 g adsorbent was added. Once the shaking process was completed, the pH values were measured [18]. The pH_{pzc} was accepted as where the initial pH

value and the final pH value were equal and recorded as 4 for Fe_3O_4 and 7 for $\text{Fe}_3\text{O}_4@HA$. HAs mainly consist of phenol, carboxylic acid, enol, quinone and ether functional groups, but they can also contain sugar and peptides. Phenol and carboxylic groups are more common in HAs structures. The structure of the HA molecule consists of hydrophilic parts containing the OH group and hydrophobic parts containing aliphatic chains and aromatic rings. Phenol and carboxylic groups are responsible for the weak acid behaviour of HAs. Quinones are electron-accepting groups and are responsible for the production of reactive oxygen species. Quinones are reduced to semiquinones stabilized by their aromatic ring, as well as to the more stable hydroquinone. The main properties of HAs, such as solubility, pH dependence, interaction with hydrophobic groups, and metal chelation, depend on their structure, namely amphiphilicity, and the different functional groups that make up each molecule. The pH_{pzc} value of $\text{Fe}_3\text{O}_4@HA$ is estimated to vary due to the stated structural properties of HA.

RESULTS AND DISCUSSION

Characteristics of Fe_3O_4 and $\text{Fe}_3\text{O}_4@HA$

According to the morphological evaluation based on SEM images, it is seen that Fe_3O_4 and $\text{Fe}_3\text{O}_4@HA$ have similar appearances (figure 2, a and b). However, when the images were examined in detail, it was determined that the aggregation tendency was high in Fe_3O_4 and low in $\text{Fe}_3\text{O}_4@HA$. It can be seen that $\text{Fe}_3\text{O}_4@HA$ did not have a uniform regular structure. Similar results were obtained in the literature [18, 19]. As a result of EDX, the % distribution of the chemical structure of Fe_3O_4 and $\text{Fe}_3\text{O}_4@HA$ was evaluated. Accordingly, Fe_3O_4 and $\text{Fe}_3\text{O}_4@HA$ contain 29.61% and 20.65% Fe, respectively. $\text{Fe}_3\text{O}_4@HA$ contains 9.17% C, which is due to HA. The FT-IR spectrum for magnetic nanoparticles is shown in figure 2, c. A broad peak between 3500 cm^{-1} and 3000 cm^{-1} was observed on both spectras of Fe_3O_4 and $\text{Fe}_3\text{O}_4@HA$ that was attributed to the O-H groups. The noteworthy peak at 1423 cm^{-1} seen on $\text{Fe}_3\text{O}_4@HA$ was associated with the vibration of C-H groups [17]. The peaks that appeared below 700 cm^{-1} were associated with Fe-O bonds in iron oxides [9, 20–21]. Fe_3O_4 and $\text{Fe}_3\text{O}_4@HA$ showed a significant peak at 548 cm^{-1} and 552 cm^{-1} , respectively, which indicated the existence of Fe-O bonds in both samples. As seen in figure 2, d, peaks expressing 35.38° (311) and 62.73° (440) crystal planes were observed in the XRD diffraction pattern of Fe_3O_4 nanoparticles. The presence of characteristic peaks indicated that Fe_3O_4 nanoparticles had been successfully synthesized. $\text{Fe}_3\text{O}_4@HA$ had similar diffraction peaks to Fe_3O_4 , which was consistent with the reverse cubic spinel structure [8]. $\text{Fe}_3\text{O}_4@HA$ ($130.7\text{ m}^2/\text{g}$) had a higher BET surface area than Fe_3O_4 ($87.6\text{ m}^2/\text{g}$). The average pore diameter for Fe_3O_4 was 5.66 nm, while the mean pore diameter for $\text{Fe}_3\text{O}_4@HA$ was 3.49 nm.

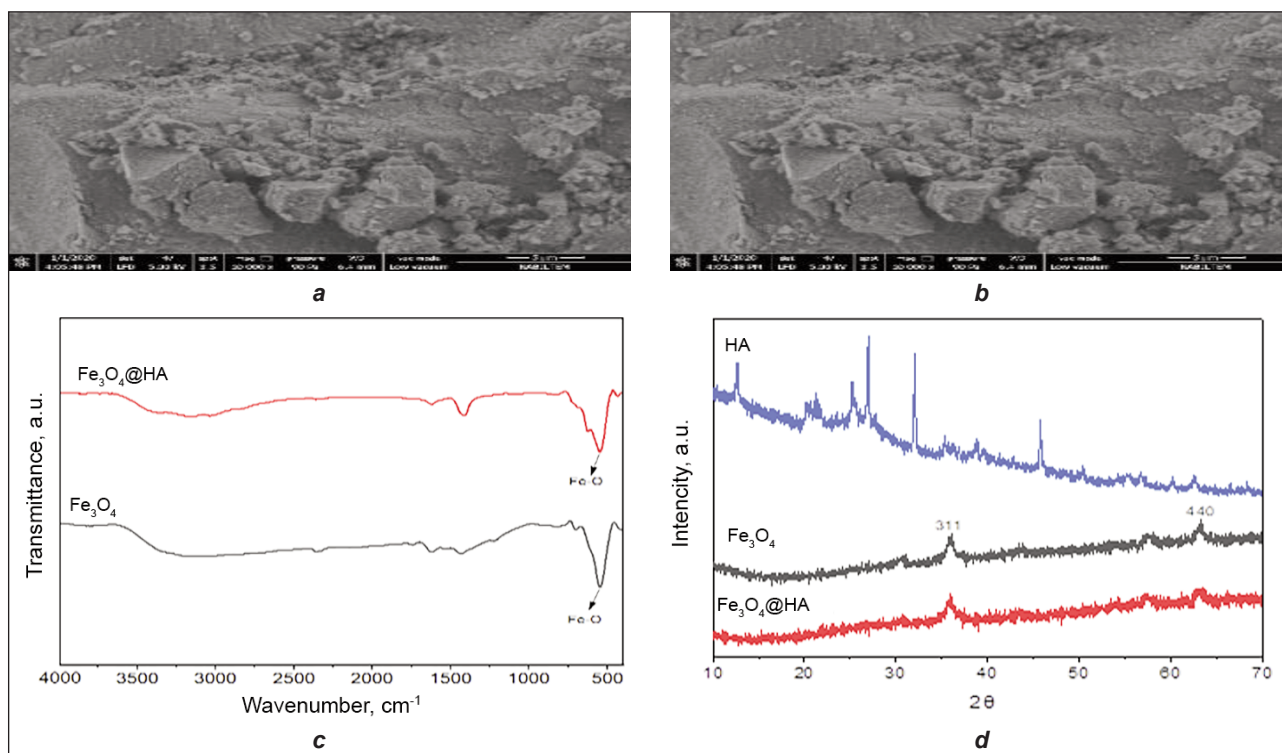


Fig. 2. Characterization of magnetic nanoparticles:
 a – SEM image of Fe_3O_4 ; b – SEM image of $\text{Fe}_3\text{O}_4@HA$; c – FT-IR; d – XRD

BET surface areas decreased with the increase in the pore diameter and increased with the decrease in the pore diameter. The pH_{pzc} values were determined as 4 and 7 for Fe_3O_4 and $\text{Fe}_3\text{O}_4@HA$, respectively.

The Effect of pH, initial dye concentration, and contact time on adsorption

The effect of pH was investigated for the use of 2 g adsorbents for $C_0 = 10$ mg AR114/l. In the literature, it was stated that iron nanoparticles dissolve below pH 2 [21], while $\text{Fe}_3\text{O}_4@HA$ dissolves above pH 12 and deteriorates structurally [6]. For this reason, the effect of pH on the adsorption capacity was evaluated for the pH values of 4, 7, and 9 and the original pH (without pH correction, 6.4). The highest q_e value (3.4 mg/g) for Fe_3O_4 was obtained at the original pH value, while the highest q_e value (3.1 mg/g) for $\text{Fe}_3\text{O}_4@HA$ was obtained at pH 4. It was stated by Koesnarpadi et al. (2017) [8] that the amount of HA used in the preparation of $\text{Fe}_3\text{O}_4@HA$ affected the adsorption capacity and increased with the increase in the amount of HA. The pH value with the highest q_e values was accepted as the optimum pH, and this pH value was taken into account in the kinetic and isotherm studies. The point of zero charges (pH_{pzc}) is the pH value at which the surface charge of the adsorbent is zero, and it is an important parameter to reveal the adsorption state of anions and cations. pH_{pzc} supports the identification of the adsorption mechanism. The pH_{pzc} values of the Fe_3O_4 and $\text{Fe}_3\text{O}_4@HA$ were determined as 4 and 7, respectively. It is known that in the case of $\text{pH} > \text{pH}_{pzc}$, the surface of the adsorbent is negatively charged [22].

For this reason, successful results could not be obtained with Fe_3O_4 at high pH values in the removal of AR114, a complex adsorption mechanism could be effective for both adsorbents in AR114 adsorption which is an anionic dye, and its q_e values are low. HA is usually negatively charged. Ligand exchange may be occurred between the anionic dye and the adsorbent surface [23]. For this reason, it is thought that better removal is achieved at pH values above the pH_{pzc} value in the adsorption of Fe_3O_4 and AR114 dyestuff. The fact that this does not happen with $\text{Fe}_3\text{O}_4@HA$ may be due to the stability that may occur with the binding of HA. The equilibrium state for both adsorbents was reached after 60 minutes. The effect of initial dye concentration on the adsorption of AR114 for both adsorbents is shown in figure 3. With the increase of the initial dyestuff concentration (from 4 mg/l to 15 mg/l), q_e (mg/g) values also increased. With the increase in the initial dye concentration, the q_e value for Fe_3O_4 increased from 0.9 mg/g to 5.34 mg/g and for $\text{Fe}_3\text{O}_4@HA$ from 0.64 mg/g to 3.1 mg/g. The initial dye concentration provides the driving force for mass transport to the adsorbent surface. The increase in dye concentration increases the driving force and the q_e value increases [24]. It was observed that when the dyestuff concentration was more than 10 mg/l, the q_e value decreased from 3.1 mg/g to 3 mg/g for $\text{Fe}_3\text{O}_4@HA$. This situation can be explained by the decrease in the regions of $\text{Fe}_3\text{O}_4@HA$ that can bind dyestuffs and the presence of low-energy binding regions.

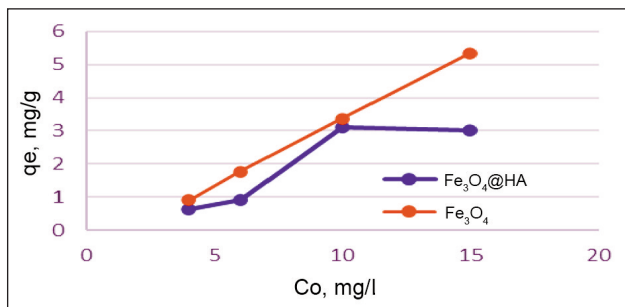


Fig. 3. Effect of initial dye concentration (Original pH (6,4), $m = 2$ g, $t = 60$ min for Fe_3O_4 , pH 4, $m = 2$ g, $t = 60$ min for $\text{Fe}_3\text{O}_4@HA$, $V = 1$ l)

Adsorption isotherms

Adsorption equilibrium studies were performed at initial concentrations between 4 mg/l and 15 mg/l, for 60 min and with 2 g adsorbents to 1 l MB solution. Isotherm studies were carried out under optimum pH conditions (pH 6.4 for Fe_3O_4 and pH 4 for $\text{Fe}_3\text{O}_4@HA$). In adsorption equilibrium studies, the maximum adsorption capacity was determined by Langmuir and Freundlich isotherm models. Equations of Langmuir and Freundlich isotherm models are given in equations 2 and 3, respectively.

$$q_e = \frac{q_{max}K_L C_e}{1 + K_L \cdot C_e} \quad (2)$$

$$q_e = K_F \cdot C_e^{1/n} \quad (3)$$

In these equations, q_{max} and q_e (mg/g) represent the maximum adsorption capacity and the adsorption capacity at equilibrium, respectively. K_L (l/mg), K_F ((mg/g)(l/mg) $^{1/n}$) and $1/n$ values are Langmuir and Freundlich parameters. In the adsorption of AR114 with Fe_3O_4 and $\text{Fe}_3\text{O}_4@HA$, q_{max} and K_L values for Langmuir isotherm, K_F and $1/n$ values for Freundlich isotherm and regression coefficients (R^2) for both isotherms are given in table 1. When the R^2 values for the adsorption of AR114 with Fe_3O_4 and $\text{Fe}_3\text{O}_4@HA$ are examined, it can be seen that the Freundlich isotherms are suitable. The R^2 values for Fe_3O_4 and $\text{Fe}_3\text{O}_4@HA$ were determined as 0.69, 0.95 and 0.52, 0.95 for Langmuir and Freundlich, respectively. The constants determined for the Freundlich isotherm are given in table 1 (constants are not given for Langmuir isotherm since the R^2 value is low for Langmuir isotherm). The plots of the Freundlich isotherm are shown in figure 4.

The $1/n$ values determined for Fe_3O_4 and $\text{Fe}_3\text{O}_4@HA$ were 2.49 and 1.33, respectively. If n is $1 < n < 10$, it can be stated that there is a compatibility between adsorbate and adsorbent. In this case, there was a strong interaction between adsorbate and adsorbent. It can be said that the adsorption mechanism was chemisorption. In this study, n values were less than 1. Since the $1/n$ values were greater than 1, it can be stated that complex adsorption took place [25]. Compliance with the Freundlich isotherm showed

Table 1

CONSTANTS FOR FREUNDLICH ISOTHERMS (Original pH (6.4), $m = 2$ g for Fe_3O_4 , $V = 1$ l, pH = 4, $m = 2$ g for $\text{Fe}_3\text{O}_4@HA$, 60 minutes, $V = 1$ l)			
Freundlich	K_f	$1/n$	R^2
Fe_3O_4	0.12	2.49	0.95
$\text{Fe}_3\text{O}_4@HA$	0.13	1.33	0.95

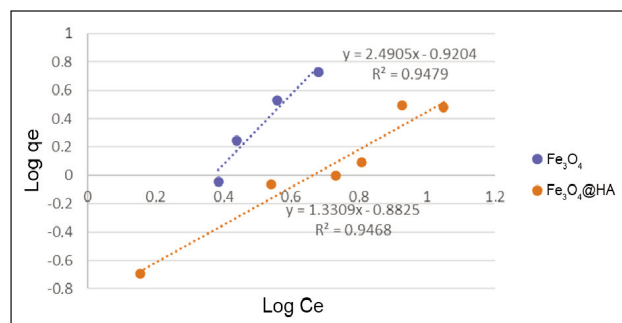


Fig. 4. Freundlich isotherm plots for the adsorption of AR114 with Fe_3O_4 and $\text{Fe}_3\text{O}_4@HA$

that the adsorbent surface had a heterogeneous structure.

Reaction kinetics

Kinetic model analyses are based on the amount of adsorbed dyestuff and contact time data. Thus, the time to reach equilibrium and the reaction rate constant can be evaluated in adsorption systems. In this study, pseudo-first order and pseudo-second order kinetic models were used to determine the adsorption kinetics. Equations of pseudo-first order and pseudo-second order kinetic models are given in equations 4 and 5, respectively.

$$q_t = q_e(1 - e^{-k_1 t}) \quad (4)$$

$$q_t = \frac{k_2 q_e^2 t}{1 + k_2 q_e t} \quad (5)$$

where q_e (mg/g) and q_t (mg/g) represent the dye uptake at equilibrium and at time t , respectively. k_1 (1/min) and k_2 (g/mg·min) are reaction rate constants. The results of the evaluation made to explain the adsorption kinetic model are given in table 2 and figure 5. According to table 2, the R^2 values of the pseudo-first-order reaction kinetics were determined as 0.9379 and 0.9493 for Fe_3O_4 and $\text{Fe}_3\text{O}_4@HA$, respectively. Likewise, the R^2 values of the second-order reaction kinetics were determined as 0.9977 and 0.9928 for Fe_3O_4 and $\text{Fe}_3\text{O}_4@HA$, respectively. When the R^2 values were examined, it was seen that the pseudo-second-order kinetic model explained the adsorption kinetics better for both adsorbents. In addition, when the calculated equilibrium adsorption capacities ($q_{e,calc}$) in pseudo-second-order model were examined, it was seen that they were quite compatible with the experimental adsorption capacities ($q_{e,exp}$). Accordingly, it can be stated that the

Table 2

KINETIC PARAMETERS FOR THE ADSORPTION OF AR114 ON Fe ₃ O ₄ AND Fe ₃ O ₄ @HA (C ₀ = 10 mg/l, pH = 6.4, m = 2 g for Fe ₃ O ₄ , V = 1 l, t = 60 min and C ₀ = 6 mg/l, pH = 4, m = 4 g for Fe ₃ O ₄ @HA, V = 1 l, t = 60 min)				
Pseudo-first order model				
Substance	q _e ^{exp} (mg/g)	q _e ^{cal} (mg/g)	k ₁	R ²
Fe ₃ O ₄	5.31	1.10	0.0336	0.9379
Fe ₃ O ₄ @HA	2.17	1.22	0.0393	0.9493
Pseudo-second order model				
Substance	q _e ^{exp} (mg/g)	q _e ^{cal} (mg/g)	k ₂	R ²
Fe ₃ O ₄	5.31	5.36	0.129	0.9977
Fe ₃ O ₄ @HA	2.17	2.23	0.157	0.9928

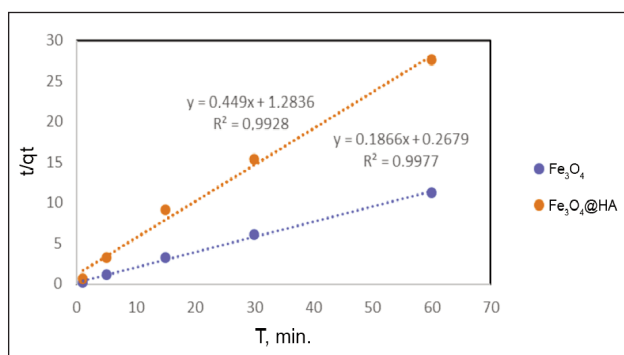


Fig. 5. Plot of pseudo-second order equation for adsorption of AR114 on Fe₃O₄ and Fe₃O₄@HA (C₀ = 10 mg/l, pH = 6.4, m = 2 g, V = 1 l, t = 60 min for Fe₃O₄ and C₀ = 6 mg/l, pH = 4, m = 4 g, V = 1 l, t = 60 min for Fe₃O₄@HA)

rate-limiting step was chemisorption and the adsorption mechanism depended on both the adsorbate and the adsorbent [26]. While the adsorption rate (k_2) for Fe₃O₄ was 0.129 mg/g·min, the k_2 value for Fe₃O₄@HA was determined as 0.157 mg/g·min.

Reuse experiments

It is economically important that the adsorbents used in adsorption studies can be reused after being regenerated. The most important advantage that dis-

tinguishes magnetic nanoparticles from other adsorbents is that they can be recycled and reused. Figure 6 shows the q_e (mg/g) values obtained after reuse. While the q_e value obtained for Fe₃O₄ (C₀ = 10 mg/l, m = 2 g, V = 1 L, pH = 6.4 and 60 min) in the first use was determined as 3.45 mg/g, at the end of the 5th use, the q_e value decreased to 2.7 mg/g. After the 7th use, the q_e value decreased to 1.5 mg/g. For Fe₃O₄@HA (m = 2 g, V = 1 l, C₀ = 4 mg/l, pH = 4 and 60 min), the q_e value was determined as 0.6 mg/g in the first use, and a decrease in the q_e value was observed after the second use. After the 6th use, the q_e value decreased to approximately 0.11 mg/g. According to the results, it was determined that Fe₃O₄ was more successful in terms of reuse than Fe₃O₄@HA and that it could be used 5 times without a significant decrease in the adsorption capacity of Fe₃O₄. This can be explained by the fact that HA in the Fe₃O₄@HA structure is an organic material, so it cannot remain as stable as Fe₃O₄ during reuse.

CONCLUSION

In this study, the removal of AR114 from aqueous solutions was investigated by batch adsorption experiments by synthesizing Fe₃O₄ and Fe₃O₄@HA. The optimum pH values determined for Fe₃O₄ and Fe₃O₄@HA were the original pH (6.4) and 4, respectively. The equilibrium state was reached after 60 minutes for both adsorbents. q_e values for Fe₃O₄ and Fe₃O₄@HA were determined with 10 mg/l initial dyestuff concentration and 2 g adsorbents as 3.4 mg/g and 3.1 mg/g, respectively. It was determined that the results obtained in the adsorption experiments performed for both adsorbents were compatible with the Freundlich isotherm and pseudo-second-order kinetic model. It was also determined that Fe₃O₄ was more efficient in terms of reuse than Fe₃O₄@HA and that Fe₃O₄ could be used 5 times without any significant loss of adsorption capacity. As a result, it can be stated that Fe₃O₄ and Fe₃O₄@HA are alternative environmentally friendly adsorbents that can be used in the removal of hazardous azo dyestuffs from water, with regeneration possibility.

ACKNOWLEDGEMENTS

This research was funded by NKU-BAP Project no: NKUBAP.06.GA.19.211.

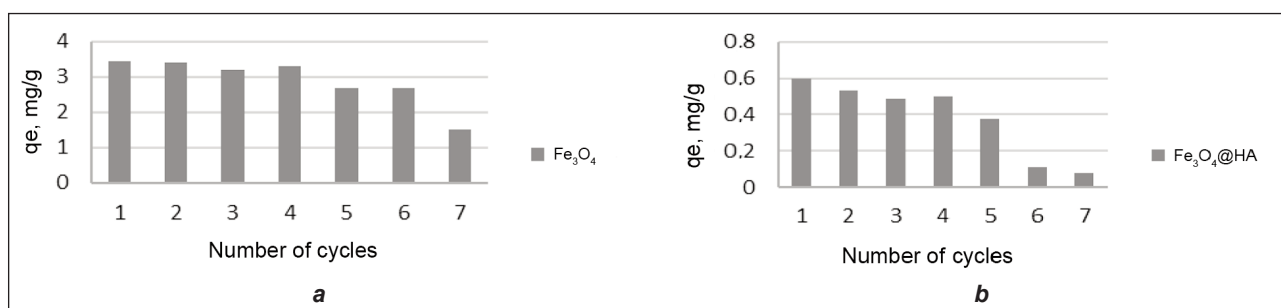


Fig. 6. q_e values depending on the number of reuses after desorption: a) Fe₃O₄ (C₀ = 10 mg/l, m = 2 g, original pH (6.4), 60 min, V = 1 l), b) Fe₃O₄@HA (C₀ = 4 mg/l, m = 2 g, pH = 4, 60 min, V = 1 l)

REFERENCES

- [1] Rapo, E., Tonk, S., *Factors Affecting Synthetic Dye Adsorption; Desorption Studies: A Review of Results from the Last Five Years (2017–2021)*, In: *Molecules*, 2021, 26, 5419, <https://doi.org/10.3390/molecules26175419>
- [2] Mani, A., Hameed, S.A.S., *Improved bacterial-fungal consortium as an alternative approach for enhanced decolourisation and degradation of azo dyes: a review*, In: *Nat. Environ. Poll. Technol.*, 2019, 18, 1, 49–64
- [3] Hu, J., Chen, G., Lo, I.M.C., *Selective removal of heavy metals from industrial wastewater using maghemite nanoparticle: performance and mechanisms*, In: *Journal of Environmental Engineering*, 2006, 132, 7, 709–715
- [4] Pan, Z., Li, W., Fortner, J.D., Giammar, D.E., *Measurement and surface complexation modeling of U(VI) adsorption to engineered iron oxide nanoparticles*, In: *Environ. Sci. Technol.*, 2017, 51, 9219–9226, <https://doi.org/10.1021/acs.est.7b01649>
- [5] Hong, H.-J., Jeong, H.S., Kim, B.-G., Honga, J., Park, I.-S., Ryu, T., Chung, K.-S., Kim, H., Ryu, J., *Highly stable and magnetically separable alginate/Fe₃O₄ composite for the removal of strontium (Sr) from seawater*, In: *Chemosphere*, 2016, 165, 231–238, <https://doi.org/10.1016/j.chemosphere.2016.09.034>
- [6] Zhang, X., Zhang, P., Wu, Z., Zhang, L., Zeng, G., Zhou, C., *Adsorption of methylene blue onto humic acid-coated Fe₃O₄ nanoparticles*, In: *Colloids and Surfaces A: Physicochem. Eng. Aspects*, 2013, 435, 85–90, <https://doi.org/10.1016/j.colsurfa.2012.12.056>
- [7] Rashid, M., Price, N.T., Pinilla, M.A.G., O'Shea, K.E., *Effective removal of phosphate from aqueous solution using humic acid coated magnetite nanoparticles*, In: *Water Research*, 2017, 123, 353–360, <https://doi.org/10.1016/j.watres.2017.06.085>
- [8] Koesnarpadi, S., Santosa, S.J., Siswanta, D., Rusdiarso, B., *Humic Acid Coated Fe₃O₄ Nanoparticle for Phenol Sorption*, In: *Indones. J. Chem.*, 2017, 17, 2, 274–283, <https://doi.org/10.22146/ijc.22545>
- [9] Rahmayanti, M., Yunita, E., Putri, N.F.Y., *Study of Adsorption-Desorption on Batik Industrial Dyes (Naphthol Blue Black) on Magnetite Modified Humic Acid (HA-Fe₃O₄)*, In: *Jurnal Kimia Sains dan Aplikasi*, 2020, 23, 7, 244–248, <https://doi.org/10.14710/jksa.23.7.244-248>
- [10] Lin, S., Shi, M., Wang, Q., Yang, J., Zhang, G., Liu, X., Fan, W., *Transport of Cu²⁺ in Unsaturated Porous Medium with Humic Acid/Iron Oxide Nanoparticle (Fe₃O₄) Amendment*, In: *Water*, 2021, 13, 200, 1–14, <https://doi.org/10.3390/w13020200>
- [11] Wan, K., Wang, G., Xue, S., Xiao, Y., Fan, J., Li, L., Miao, Z., *Preparation of Humic Acid/L-Cysteine-Codecorated Magnetic Fe₃O₄ Nanoparticles for Selective and Highly Efficient Adsorption of Mercury*, In: *ACS Omega*, 2021, 6, 7941–7950, <https://doi.org/10.1021/acsomega.1c00583>
- [12] Peng, L., Qin, P., Lei, M., Zeng, Q., Song, H., Yang, J., Shao, J., Liao, B., Gu, J., *Modifying Fe₃O₄ nanoparticles with humic acid for removal of Rhodamine B in water*, In: *Journal of Hazardous Materials*, 2012, 209–210, 193–198, <https://doi.org/10.1016/j.jhazmat.2012.01.011>
- [13] Amir, Md., Güner, S., Yıldız, A., Baykal, A., *Magneto-optical and catalytic properties of Fe₃O₄@HA@Ag magnetic nanocomposite*, In: *Journal of Magnetism and Magnetic Materials*, 2017, 421, 462–471, <https://doi.org/10.1016/j.jmmm.2016.08.037>
- [14] National Institutes of Health (NIH) – PubChem, *Compound Summary C.I. Acid Red 114*, Available at: <https://pubchem.ncbi.nlm.nih.gov/compound/C.I.-Acid-Red-114> [Accessed on December 2022]
- [15] Welham, A.C., *Wool Dyeing*, UK Patent GB 2 236 767 A, 1991, Available at <https://patentimages.storage.googleapis.com/3b/ec/ed/57aedbe44c0d35/GB2236767A.pdf> [Accessed on December 2022]
- [16] Damasceno, B.S., Viana Da Silva, A.F., Vaz de Araujo, A.C., *Dye adsorption onto magnetic and superparamagnetic Fe₃O₄ nanoparticles: A detailed comparative study*, In: *Journal of Environmental Chemical Engineering*, 2020, 8, 103994, <https://doi.org/10.1016/j.jece.2020.103994>
- [17] Yıldız, A., Güneş, E., Amir, Md., Baykal, A., *Adsorption of industrial Acid Red 114 onto Fe₃O₄@Histidine magnetic nanocomposite*, In: *Desalination and Water Treatment*, 2017, 60, 261–268, <http://dx.doi.org/10.5004/dwt.2017.0295>
- [18] Santos, S.C.R., Vilar, V.J.P., Boaventura, R.A.R., *Waste metal hydroxide sludge as adsorbent for a reactive dye*, In: *Journal of Hazardous Materials*, 2008, 153, 3, 999–1008, <http://10.1016/j.jhazmat.2007.09.050>
- [19] Singhal, P., Jha, S.K., Pandey, S.P., Neogy, S., *Rapid extraction of uranium from sea water using Fe₃O₄ and humic acid coated Fe₃O₄ nanoparticles*, In: *Journal of Hazardous Materials*, 2017, 335, 152–161, <https://doi.org/10.1016/j.jhazmat.2017.04.043>
- [20] Azizi, A., *Green Synthesis of Fe₃O₄ Nanoparticles and Its Application in Preparation of Fe₃O₄/Cellulose Magnetic Nanocomposite: A Suitable Proposal for Drug Delivery Systems*, In: *Journal of Inorganic and Organometallic Polymers and Materials*, 2020, 30, 3552–3561, <https://doi.org/10.1007/s10904-020-01500-1>
- [21] Absalan, G., Asadi, M., Kamran, S., Sheikhan, L., Goltz, D.M., *Removal of reactive red-120 and 4-(2-pyridylazo) resorcinol from aqueous samples by Fe₃O₄ magnetic nanoparticles using ionic liquid as modifier*, In: *Journal of Hazardous Materials*, 2011, 192, 476–484, <https://doi.org/10.1016/j.jhazmat.2011.05.046>
- [22] Lu, H., Wang, J., Li, F., Huang, X., Tian, B., Hao, H., *Highly Efficient and Reusable Montmorillonite/Fe₃O₄/Humic Acid Nanocomposites for Simultaneous Removal of Cr(VI) and Aniline*, In: *Nanomaterials*, 2018, 8, 7, 537, <https://doi.org/10.3390/nano8070537>
- [23] Xu, J., Wu, P., Ye, E., Yuan, B., Feng, Y., *Metal oxides in sample pretreatment*, In: *TrAC Trends in Analytical Chemistry*, 2016, 80, 41–56, <https://doi.org/10.1016/j.trac.2016.02.027>

- [24] Kaykioğlu, G., Güneş, E., *Kinetic and equilibrium study of methylene blue adsorption using H₂SO₄-activated rice husk ash*, In: Desalination and Water Treatment, 2016, 57, 15, 7085–7097, <https://doi.org/10.1080/19443994.2015.1014859>
- [25] Foo, K.Y., Hameed, B.H., *Utilization of rice husk ash as novel adsorbent: a judicious recycling of the colloidal agricultural waste*, In: Advances in Colloid and Interface Science, 2009, 152, 1–2, 39–47, <http://dx.doi.org/10.1016/yj.cis.2009.09.005>
- [26] Ertugay, N., Malkoc, E., *Adsorption Isotherm, Kinetic, and Thermodynamic Studies for Methylene Blue from Aqueous Solution by Needles of Pinus Sylvestris L.*, In: Pol. J. Environ. Stud., 2014, 23, 6, 1995–2006
-

Authors:

GÜL KAYKIOĞLU¹, DERMAN VATANSEVER BAYRAMOL², AYLIN YILDIZ³

¹Department of Environmental Engineering, Faculty of Corlu Engineering, Tekirdag Namik Kemal University, 59860 Corlu, Tekirdag, Türkiye

²Department of Metallurgy and Materials Engineering, Faculty of Engineering, Alanya Alaaddin Keykubat University, Alanya, Antalya, Türkiye
e-mail: derman.bayramol@alanya.edu.tr

³Department of Textile Engineering, Faculty of Corlu Engineering, Tekirdag Namik Kemal University, 59860 Corlu, Tekirdag, Türkiye
e-mail: ayildiz@nku.edu.tr

Corresponding author:

GÜL KAYKIOĞLU
e-mail: gkaykioglu@nku.edu.tr